minerals

MDPI

Article

Stable Isotope ($\delta^{18}O$, δD) Composition of Magmatic Fluids Exsolved from an Active Alkaline Magma Chamber—The Case of the AD 79 Magma Chamber of Vesuvius

Paolo Fulignati [1,*] and Adrian J. Boyce [2]

[1] Dipartimento di Scienze della Terra, Via S. Maria 53, 56126 Pisa, Italy
[2] Scottish Universities Environmental Research Centre, Rankine Ave, East Kilbride, Glasgow G75 0QF, UK; adrian.boyce@glasgow.ac.uk
* Correspondence: paolo.fulignati@unipi.it

Abstract: This work documents, for the first time, the calculated oxygen and hydrogen isotope composition of the brines exsolved from the peripheral margin of the active magma alkaline chamber that fed the AD 79 ("Pompei") eruption of Vesuvius. The exsolved hydrosaline fluids had a constant $\delta^{18}O$ composition and a variable δD composition, showing a general lowering of δD at nearly constant $\delta^{18}O$ content. We argue that the progressive fluid exsolution at the upper peripheral parts of the AD 79 magma chamber may explain this isotopic path. The modeling of the evolution of the hydrogen isotope composition of water remaining dissolved in the melt, and of the exsolved fluid as a consequence of progressive degassing, would favor multiple fluid-release events from the magmatic reservoir. A schematic model on the pulsed accumulation and release of fluids at the top of the magmatic reservoir prior to the eruption is thus proposed. The assessment of the stable isotope composition of the fluids exsolved from the AD 79 magma chamber of Vesuvius may be particularly relevant for the geochemical surveillance of the volcano as it may help to interpret the isotopic composition of fumarolic gases and its variations.

Keywords: Vesuvius; AD 79 eruption; stable isotopes; magmatic fluids; brines; fluid exsolution

Citation: Fulignati, P.; Boyce, A.J. Stable Isotope ($\delta^{18}O$, δD) Composition of Magmatic Fluids Exsolved from an Active Alkaline Magma Chamber—The Case of the AD 79 Magma Chamber of Vesuvius. *Minerals* **2023**, *13*, 913. https://doi.org/10.3390/min13070913

Received: 2 June 2023
Revised: 30 June 2023
Accepted: 4 July 2023
Published: 6 July 2023

1. Introduction

Most magmas become saturated in volatiles and exsolve a free fluid phase(s) during their evolution in the shallow crust. This commonly results in the generation of an aqueous magmatic fluid (Edmonds and Wood [1] and reference therein). The exsolution of magmatic fluids from crystallizing silicate melt is a fundamental process, which strongly influences the physical and chemical properties of magmas in the subsurface environment, resulting in large-scale geologic phenomena that have major societal and economic implications. These phenomena include: the release of climate-altering gases into the atmosphere [2], the control on the explosivity of volcanic eruptions [3] and the generation of economically important magmatic-hydrothermal ore deposits [4,5]. The exsolution of magmatic fluids is in fact pivotal in the partitioning of ore metals from melt to a hydrothermal system and the subsequent precipitation and concentration of metals [5–7].

The evolution of an immiscible aqueous fluid phase from magmas typically takes place in the poorly characterized interval between the orthomagmatic and hydrothermal regimes, which has proved extremely difficult to document due to the transient reactive nature of the exsolved volatile phases [4,8]. As a consequence, although of crucial importance for many geological processes, as reported above, direct measurements of the chemical and isotopic composition of magma-derived fluids are not easy to obtain, and their knowledge mostly derives from the study of fumarolic emissions of active volcanoes (Fischer and Chiodini [9] and references therein). In that case, however, the composition of fluids can be mediated by fluid–rock interaction processes and by possible contamination with

shallow waters. The rare opportunity where we can obtain direct measurements on the original composition of magmatic fluids, is offered by the investigation of fluid inclusions entrapped within crystals (from the juvenile fraction and/or cognate xenoliths) ejected during volcanic eruptions [10–18]. Fluid inclusions therefore, represent in many cases the only direct witness of the exsolved fluid, and their investigation is pivotal to determine the chemical and isotopic composition of the fluids released by an active magma chamber [17].

The present study was undertaken to document, for the first time, the oxygen and hydrogen isotope composition of the brines exsolved from the peripheral margin of an active magma chamber, as deduced from the investigation of minerals and decrepitated fluid inclusions in cognate xenoliths (foid-bearing syenites) representing the upper portions of the AD 79 (Pompei) magma chamber of Vesuvius. Furthermore, we used δ18O and δD evolution of magmatic fluids to obtain inferences on the dynamic of magmatic fluid release from the AD 79 magma chamber.

2. The AD 79 Magma Chamber and Investigated Samples

The AD 79 Plinian eruption ("Pompei" eruption) of Vesuvius tapped a magma chamber located at a relatively shallow depth (3–6 km) within the Mesozoic carbonate basement [19–22]. Previous studies [20,21] hypothesized the AD 79 magma chamber to be characterized by a subequant shape and a main twofold layering, with a stepwise gradient separating the lower, convecting, mildly evolved portion (tephriphonolite, T = 1000–1100 °C) from the upper, statically stratified, and volatile-rich (H_2O, Cl, F) felsic portion (phonolite, T = 850–900 °C). The outer margin of the magma chamber, consisting of crystallized magma (clinpyroxenites to foid-bearing syenites), continuously grades into carbonate country rocks through a thermometamorphic and metasomatized (skarn and marbles) shell [14].

Our study focuses on foid-bearing syenite cognate xenoliths representing the solidification front [23] of the upper parts of the AD 79 magma chamber of Vesuvius. These are nearly hypoyaline, nonequigranular rocks consisting of a network of euhedral crystals of K-feldspar; other constituents are sodalite, biotite, K-pargasitic amphibole, garnet, leucite and scarce nepheline. Many accessories are also present: sphene, apatite and monazite are among the most abundant. The foamy appearance of these rocks can be interpreted to result from the crystallization of K-feldspars in the presence of exsolved fluids accumulating under the roof of the magma chamber. On the other hand, K-feldspars host abundant multiphase fluid inclusions testifying the direct exsolution of a hydrosaline aqueous fluid phase from the crystallizing upper peripheral portions of the magma chamber [14,17]. These fluid inclusions are generally primary and consist of a deformed vapor bubble + scarce liquid phase + several clear daughter minerals of cubic shape (halite and sylvite) + two or more rounded and tabular daughter minerals ± opaque crystals (Figure 1). Microthermometric experiments revealed homogenization temperatures ranging from 760° to 830 °C, with a mode at about 810 °C, and salinity in the range of 62–70 wt.% $NaCl_{equiv.}$ [17]. With the aim to characterize the isotopic composition of the fluids exsolved from the peripheral parts of the AD 79 magma chamber of Vesuvius prior to the eruption, oxygen and hydrogen isotope compositions of minerals, assumed to be in equilibrium with the exsolved magmatic fluid, and multiphase fluid inclusions (only δD) from foid-bearing syenite xenoliths were determined.

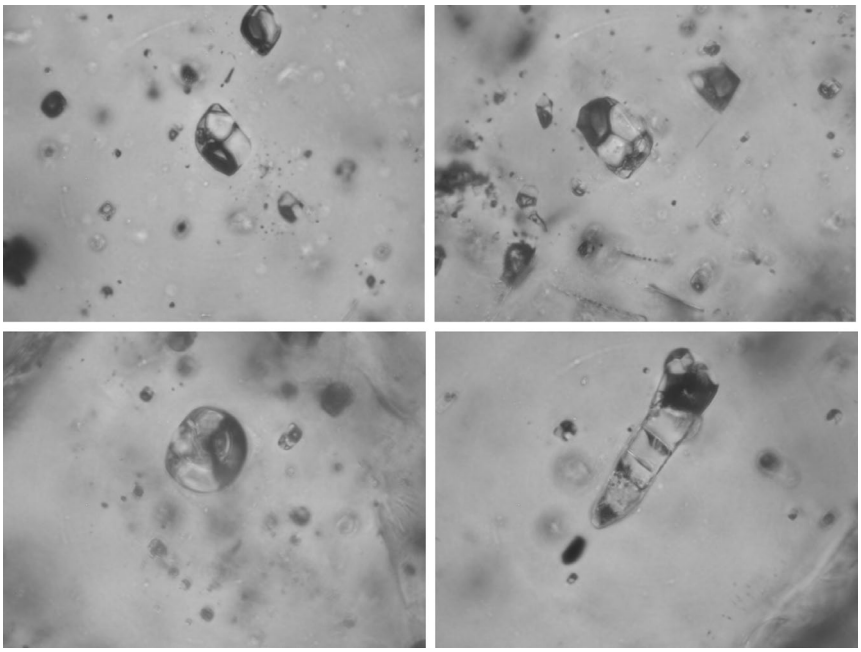

Figure 1. Microphotographs of multiphase fluid inclusions hosted within K-feldspars of foid-bearing syenite cognate xenoliths.

3. Analytical Methods

Oxygen isotope analyses on K-feldspar and biotite were carried out by laser fluorination of the total sample (typically between 1 and 2 mg) with excess ClF3 using a CO_2 laser as a heat source (T in excess of 1500 °C; [24]). All fluorinations resulted in 100% release of O_2 from the silica lattice. This O_2 was converted to CO_2 by reaction with hot graphite, then analyzed on-line by a VG PRISM III spectrometer. Reproducibility is better than ±0.3‰ (1σ) based on repeated analyses of internal lab standard quartz SES-1 (+9.6‰). For H isotope analysis of fluid inclusion water, pure K-feldspar samples (mostly between 0.5 and 2 gr), hosting hypersaline fluid inclusions, were heated to 200 °C overnight under high vacuum to release labile volatiles. In the case of biotite, outgassing was carried out on several tens of mg of pure mineral separate at 150 °C. In both cases, samples were then placed in an outgassed Pt crucible, and gradually heated by radiofrequency induction in an evacuated quartz tube to temperatures in excess of 1500 °C. The released water was then reduced to H2 in a chromium furnace at 800 °C [25], with the evolved gas measured quantitatively in a Hg manometer, then collected using a Toepler pump. The gas was subsequently analyzed on a VG 602D mass spectrometer with a manual Hg, high gas compression inlet system. Replicate analyses of water standards were used to calibrate raw data from the mass spectrometer (international std GISP, and internal standards Lt Std, LSW) and gave a standard error reproducibility better than ±3‰. Replicate analyses of international mineral standard NBS-30 (biotite) also gave reproducibility around ±2‰.

4. Results

The measured oxygen isotope compositions of K-feldspars ($\delta^{18}O$ values between 9.8‰ and 10.1‰) and biotite (8.6‰) of the juvenile fraction (Table 1) were compatible with the values reported for Vesuvian products [26,27]. The $\delta^{18}O$ values of K-feldspars and biotite of foid-bearing syenites were consistently higher than those of the juvenile fraction and ranged from 10.6‰ to 12.5‰ (K-feldspars) and 10.2‰ (biotite), respectively (Table 1). The oxygen isotopic composition of the fluid in equilibrium with K-feldspars and biotite of foid-bearing syenites was calculated using the fractionation data of Zheng [28] and Zheng [29], respectively. The equilibrium temperature was assumed to be 810 °C on the basis of fluid inclusion microthermometric results [17]. The K-feldspar–water fractionation factor was very low (about 0.1‰) considering this high equilibrium temperature, and the $\delta^{18}O$ calculated

composition of the fluid in equilibrium with these K-feldspars was in the range of 10.7–12.6‰ (Figure 2). The $\delta^{18}O$ calculated composition of fluid in equilibrium with biotite was 12.5‰ and falls in the range obtained for the fluid in equilibrium with K-feldspars.

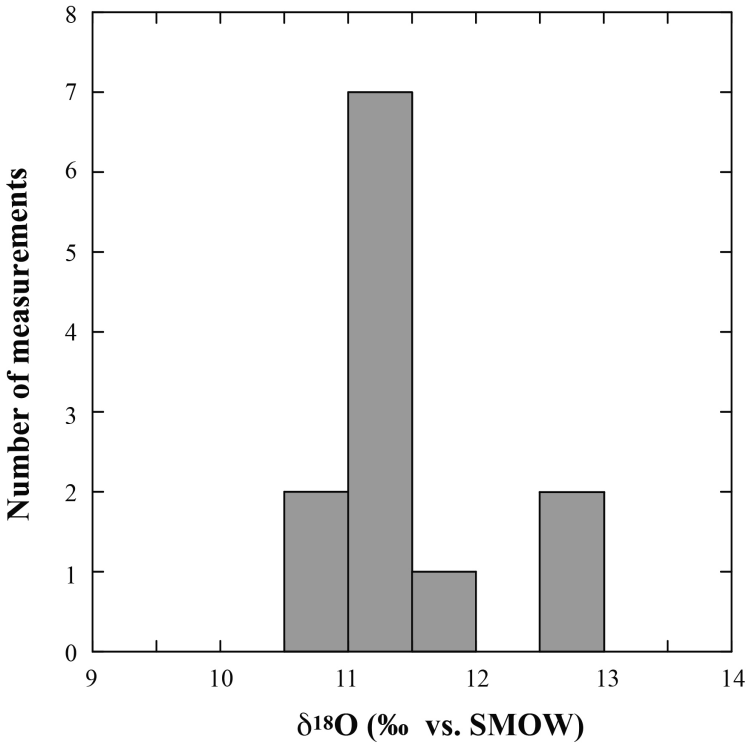

Figure 2. Frequency histogram of $\delta^{18}O$ composition of fluids in equilibrium with K-feldspar and biotite.

Table 1. Oxygen and hydrogen isotopic data of minerals and fluid inclusions, and calculated fluid compositions for waters in equilibrium with minerals at temperatures determined from fluid inclusion data.

Sample	Mineral	Rock Type	Measured		Calculated	
			$\delta^{18}O$ (‰)	δD (‰)	$\delta^{18}O$ (‰) Water	δD (‰) Water
		AD 79 eruption				
79-91	K-feldspar	foid-bearing syenite	10.6		10.7 *	
Vs95-79-7	K-feldspar	foid-bearing syenite	12.5	−90	12.6 *	−90 **
51	K-feldspar	foid-bearing syenite	11.3	−55	11.4 *	−55 **
52	K-feldspar	foid-bearing syenite	11.3	−86	11.4 *	−86 **
53	K-feldspar	foid-bearing syenite	11.3	−62	11.4 *	−62 **
54	K-feldspar	foid-bearing syenite	11.2	−90	11.3 *	−90 **
55	K-feldspar	foid-bearing syenite	11.3	−101	11.4 *	−101 **
56	K-feldspar	foid-bearing syenite	11.3	−97	11.4 *	−97 **
57	K-feldspar	foid-bearing syenite	11.7	−90	11.8 *	−90 **
71	K-feldspar	foid-bearing syenite	11.2	−99	11.3 *	−99 **
72	K-feldspar	foid-bearing syenite	10.7	−111	10.8 *	−111 **
SAN-5 bt	biotite	foid-bearing syenite	10.2	−143	12.5 *	
EU 2 K-feld	K-feldspar	juvenile fraction	10.1			
KF-79	K-feldspar	juvenile fraction	9.8			
EU 2 bt	biotite	juvenile fraction	8.6	−52		−52 ***
		AD 472 eruption				
Vs88-48	biotite	juvenile fraction	6.3	−58		−58 ***

* = calculated values from fractionation factors of: Zheng [28] (oxygen, K-feldspar), Zheng [29] (oxygen, biotite) and assuming a temperature of 810 °C as deduced from fluid inclusion study [17]. ** = measured values from decrepitated multiphase fluid inclusions. *** = δD value for igneous biotite is taken as being representative of the water dissolved in the melt since there is little fractionation between OH minerals and melt water [30]. Red = K-feldspar–biotite pair representative of the juvenile fraction reported in Figure 3. Blue = K-feldspar–biotite pair representative of the foid-bearing syenite reported in Figure 3.

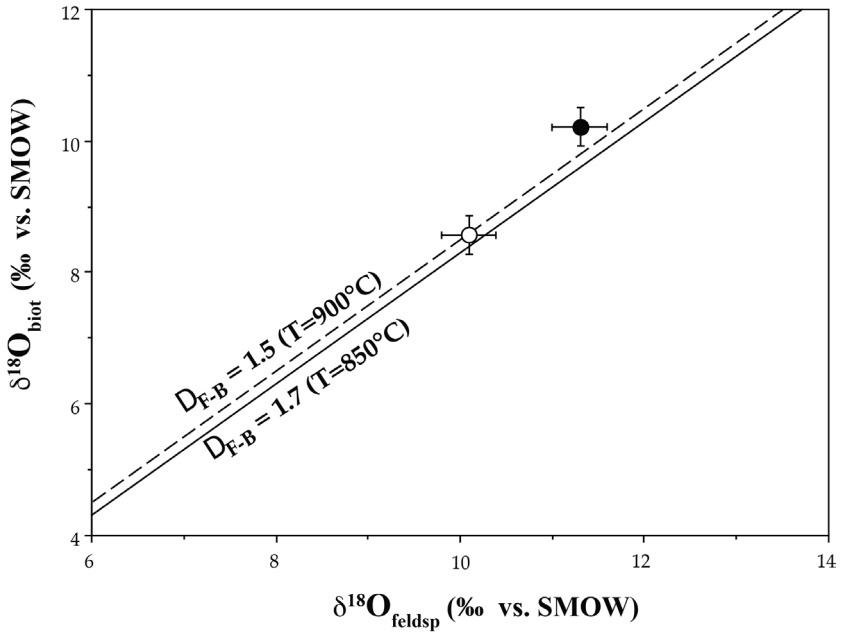

Figure 3. Diagram of $\delta^{18}O$ values of coexisting K-feldspar and biotite. White dot K-feldspar–biotite pair in juvenile fraction, black dot K-feldspar–biotite pair in foid-bearing syenite.

The δD values of water trapped in hypersaline fluid inclusions, hosted within K-feldspar from different samples of foid-bearing syenite xenoliths, are rather variable ranging from −55‰ to −111‰ (Table 1). The δD values of biotite of AD 79 and AD 472 juvenile fractions (for comparison) are −52‰ and −58‰, respectively, whereas the measured δD of biotite of foid-bearing syenite xenoliths is −143‰ (Table 1).

5. Discussion

The collected stable isotope data on minerals and fluid inclusions allow for constraining the $\delta^{18}O$ and δD composition of the fluid exsolved from the peripheral portions of the AD 79 Vesuvius magma chamber. The $\delta^{18}O$ values of the fluids in equilibrium with K-feldspar and biotite of foid-bearing syenites are in the range of 10.7–12.6‰, but most of the data are between 11.0‰ and 11.5‰ (Figure 2). These values are higher than the typical "magmatic water box" [31,32] but almost all fall close to the ^{18}O-enriched limit of the convergent margins magmatic waters (CMW) proposed by [33,34]. However, these high $\delta^{18}O$ values, and in particular the highest (12.5‰ and 12.6‰), may reflect exchange effects between magma and wall rocks at the margins of the magma chamber prior to fluid exsolution. This process is highlighted in several margins of plutons and seems to take place without any significant mineralogical or chemical change in the magmatic rocks. It appears to involve just ^{18}O exchange directly between magmatic melt and the wall rocks or by the local assimilation of the wall rocks (Taylor and Sheppard [35] and references therein).

The $\delta^{18}O$ composition of K-feldspar and biotite were also used to give an estimation of the temperature of equilibration. The fractionation equation for the K-feldspar–biotite pair ($\Delta_{feldsp\text{-}biot} = 2.5(10^6T^{-2}) - 0.31$) has been calculated by using the fractionation equations of O'Neil and Taylor [36] and Bottinga and Javoy [37,38] for K-feldspar and biotite, respectively. The oxygen isotope composition of K-feldspar and biotite of the juvenile fraction gave a temperature of equilibrium of 850–900 °C (Figure 3) that agrees very well with the temperatures estimated from melt inclusion microthermometries [20]. The $\delta^{18}O$ value of K-feldspar and biotite in foid-bearing syenites shows a per mil difference lower than that of the juvenile fraction, this would indicate higher temperatures of equilibrium that are reasonably unlikely, so $\delta^{18}O$ disequilibrium is implied instead.

The hydrogen isotopic composition of the exsolved fluids was directly measured in decrepitated multiphase fluid inclusions, which are hosted in several samples of foid-bearing

syenite xenoliths. Despite the homogeneous petrographic and microthermometric characteristics found in the various samples, fluid inclusions show a large δD range from −55‰ to −111‰ (Table 1). On a δ^{18}O-δD diagram, our data depict a trend of δD impoverishment at nearly constant δ^{18}O content for exsolved fluids (Figure 4).

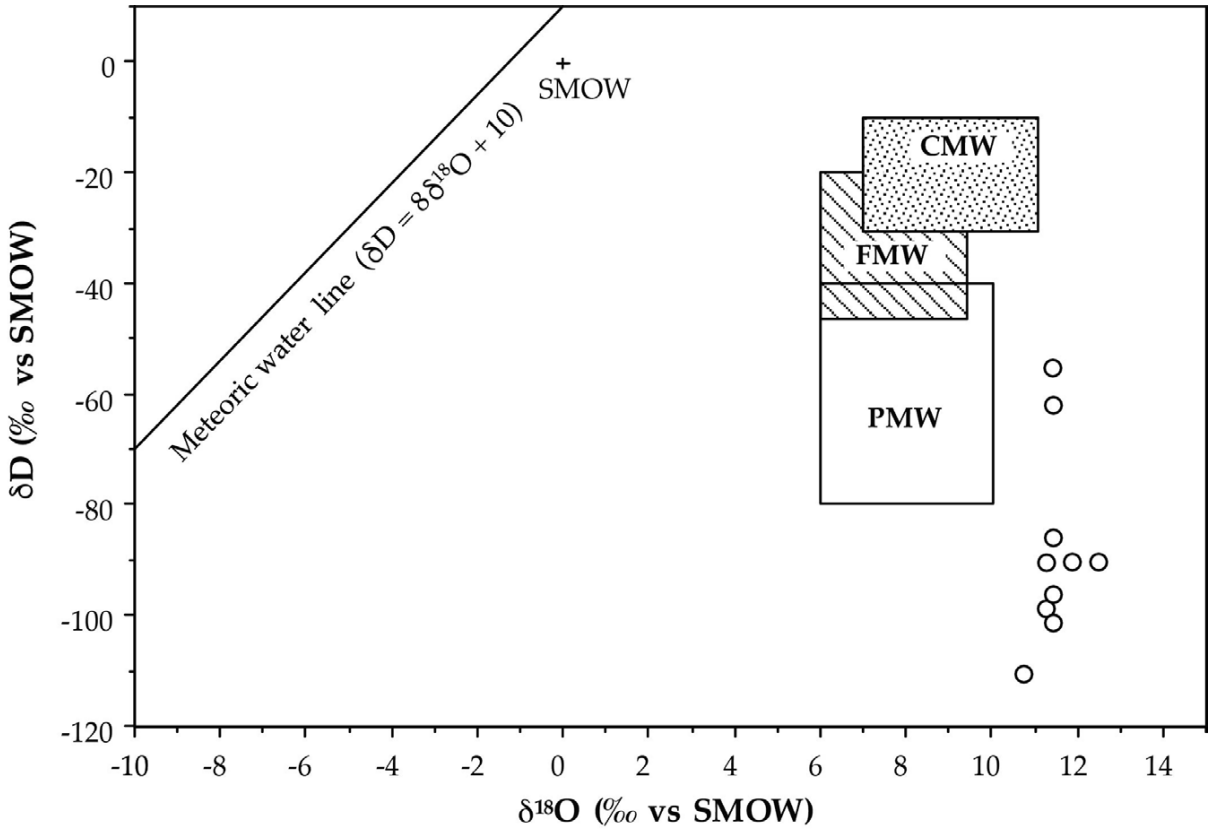

Figure 4. Calculated fluid δ^{18}O vs. measured fluid δD diagram (see Table 1) showing the oxygen and hydrogen isotopic composition of magmatic fluids exsolved at the crystallizing upper peripheral portions of the AD 79 Vesuvius magma chamber. PMW = primary magmatic water [39]; FMW = felsic magmatic water [40]; CMW = convergent margins magmatic waters [33,34].

This is very similar to what was reported in several stable isotope studies on magmatic fluids involved in potassic and phyllic alterations of porphyry copper deposits and in skarn deposits [41–44]. The highest δD values found in multiphase fluid inclusions are close to that of the juvenile biotite of AD 79 and also AD 472 Vesuvius eruptions (−52/−58‰, Table 1). These values are compatible with the δD composition of "magmatic" water proposed by Taylor [32] and Sheppard [39] and also with the δD composition of the water dissolved in felsic magmas of Taylor [40] (considering that Vesuvian magmas emplaced into continental crust), and can be assumed to represent the hydrogen isotopic composition of the water dissolved in Vesuvian magma before exsolution begins. Conversely, several δD data are lower than those assumed to be representative of the typical magmatic waters (Figure 4). Excluding the contribution of external fluids (i.e., meteoric water), one explanation for such a large δD variation is the effect of progressive degassing of the solidification front of the AD 79 magma chamber. The trend of δD impoverishment at nearly constant δ^{18}O content can in fact be explained by considering the significant hydrogen isotopic fractionation as water in a melt exsolves to the aqueous fluid phase [45]. In contrast, the δ^{18}O fractionation between water and melt is negligible at magmatic temperature [46]. Fluid inclusion evidences the direct exsolution of a hypersaline fluid phase from magma [17], and excludes that δD fractionation could be influenced by the phase separation of hypersaline liquid from vapor [47,48]. According to Dobson et al. [49] and Taylor [44,50,51], the

fractionation of hydrogen isotopes between magma and an exsolved aqueous fluid phase varies primarily as a function of the hydrogen speciation (H_2O and OH) in the melt, which varies with water content [52] and can be calculated, according to Taylor [51], as:

$$1000\ln\alpha(H_2O\text{-melt}) = XH_2O\ 10^3\ \ln\alpha H_2O-(H_2O_{melt}) + (1 - X)OH\ 10^3\ \ln\alpha H_2O-(OH_{melt}) \quad (1)$$

where X and 1 − X are, respectively, the atom fraction of hydrogen present in the melt as H_2O and OH and α is the isotopic fractionation factor. The values of $\alpha H_2O-(H_2O_{melt})$ and $\alpha H_2O-(OH_{melt})$ are 1.000 and 1.0415, respectively, as estimated by Dobson et al. [49]. The bulk fractionation factor between exsolved water and magma can therefore vary from about 0‰ to about 40‰. Thus, as water exsolves from the saturated melt, the residual melt is depleted in deuterium. The extent and rate of decrease in deuterium depend upon whether degassing is an open- or closed-system (open-system degassing leads to the largest variations in δD) process and on the ratio of H_2O and OH species in the melt [44,49–51,53]. As a consequence, Hedenquist et al. [39] argued that magmatic water, as defined by Taylor [32], is more appropriately termed residual magmatic water because it represents the water left in magma upon complete crystallization, and thus, after the majority of the water has exsolved. The progressively lighter δD water that remains in the melt, as a result of fluid exsolution, may be incorporated by hydroxyl-bearing mineral and/or degas at later stage, and become depleted in deuterium from that of the initial exsolved fluid [41]. The trend of δD impoverishment shown by Vesuvius magmatic fluids can be envisaged to be generated by this process. The fluids entrapped within inclusions found in foid-bearing syenite cognate xenoliths would record the progressive release of a magmatic aqueous fluid phase, which is progressively depleted in deuterium, from the upper peripheral crystallizing margin of the AD 79 magma chamber. The low δD values reached by these fluids (up to −111‰) sugget that the exsolution occurred (almost in part) in open-system conditions (Rayleigh fractionation). We might hypothesize that an initial closed-system degassing was followed by an open-system degassing, reflecting the shift from ductile and largely sealed conditions to brittle permeable conditions ("Closed–Open"). More probably, we envisage a more complex behavior in which the exsolved magmatic fluids (closed-system degassing) accumulated at lithostatic pressure in the roof zone [1] of the magma chamber (Figure 5a). This accumulation of fluids caused a pressure increase near the top of the zone of accumulation, resulting in hydraulic fracturing or opening of pre-existing fractures, with the consequent release of accumulated fluids (Figure 5b) from the normally plastic region into the brittle, and depressurization [54–56]. The released fluids flowed into the carbonate wall rocks producing exoskarn [14–16]. After the decrease in pressure of the accumulated fluids, the fractures were closed by mineral deposition and plastic flow (Figure 5c), and magmatic fluids again restarted to accumulate at the top of the magma chamber (new closed-system degassing stage).

This process probably recurred more times before the AD 79 Plinian eruption that disrupted the magma chamber, leading to the intermittent release of fluids (as already suggested for some porphyry systems [57,58]) that were even more depleted in deuterium. For this reason, it can be viewed as a quasi-open degassing process consisting of several closed or nearly closed stages ("Multi-Step Closed/Open"). The evolution of the hydrogen isotope composition of water remaining dissolved in the melt and of the exsolved fluid as a function of the two proposed processes ("Closed-Open" and "Multi-Step Closed/Open") is modeled in Figure 6 (see Appendix A for calculations). The results show that both processes can well explain the δD evolution of the exsolved fluids recorded in fluid inclusions of the foid-bearing syenite xenoliths (Figure 6).

The very low δD value found in biotite from the foid-bearing syenites (−143‰) may represent the isotopic composition of the residual water, after the large majority of the water has exsolved.

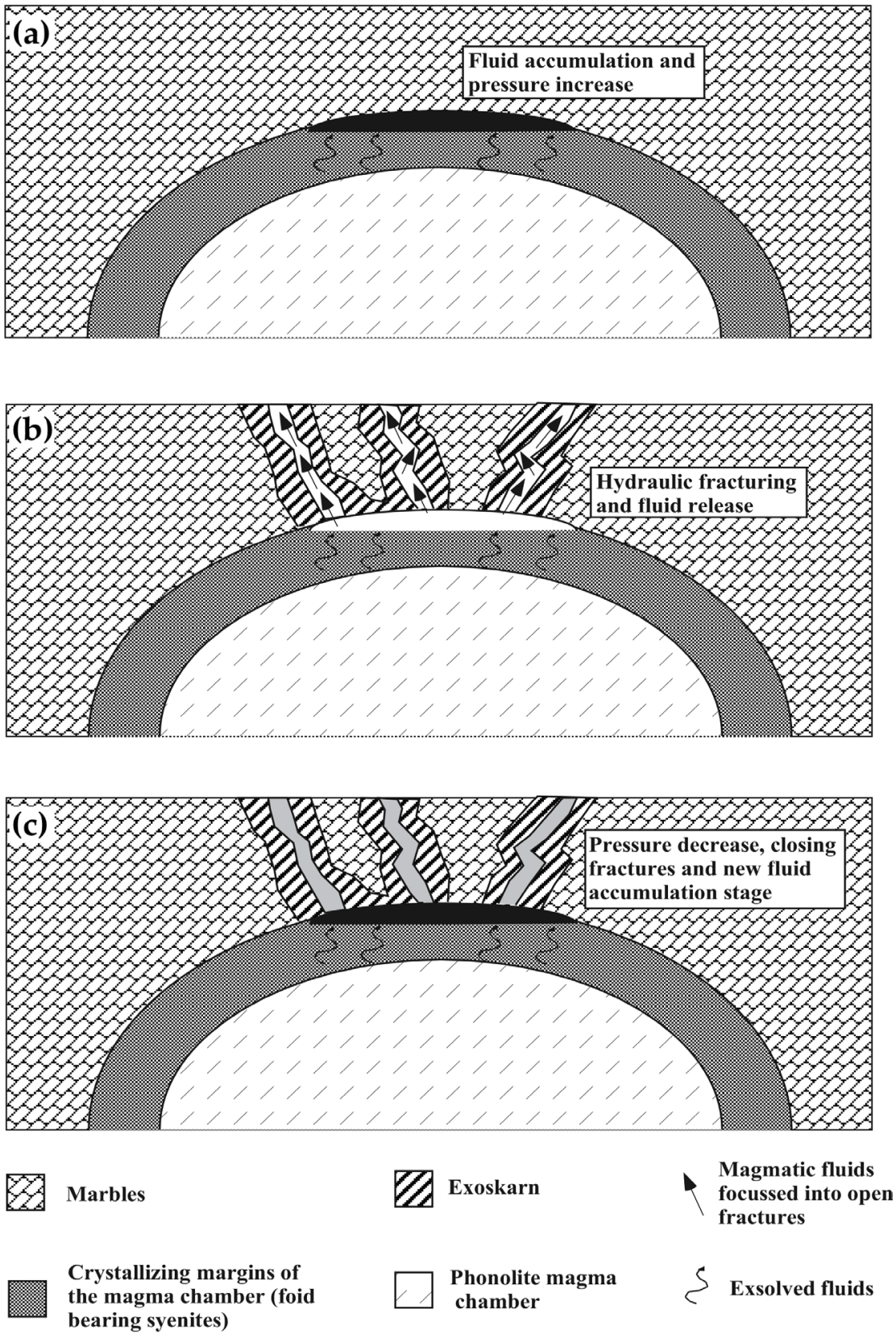

Figure 5. (**a**–**c**) Schematic sketch of the proposed Multi-Step Closed/Open degassing model at the roof of the AD 79 magma chamber of Vesuvius.

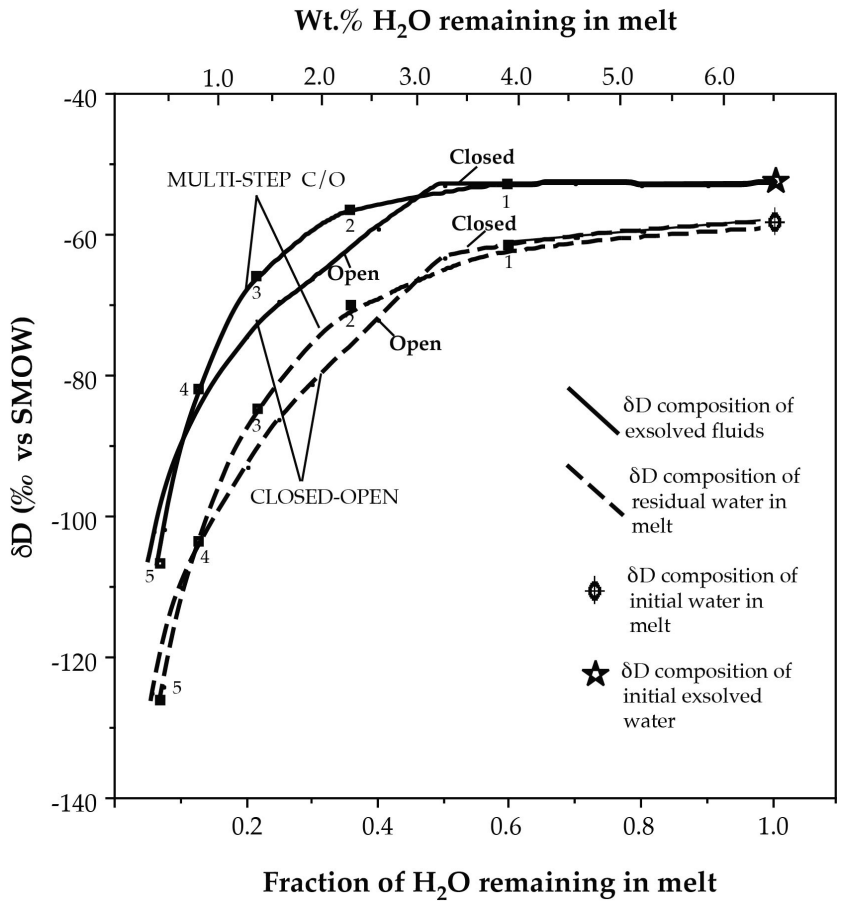

Figure 6. Plot of δD versus fraction of water remaining in melt, illustrating hydrogen isotope fractionation and variation of water content in the melt during exsolution of fluids at the roof of the AD 79 magma chamber of Vesuvius under Closed/Open system conditions and under Multi−Step Closed/Open system conditions (see Appendix A for calculation details).

6. Conclusions

This work reports for the first time the calculated stable isotope composition (oxygen and hydrogen) of the fluids directly exsolved from the peripheral margin of the active alkaline magma chamber that fed the AD 79 eruption of Vesuvius. These results show that the exsolved hydrosaline fluids had a constant $\delta^{18}O$ composition and a variable δD composition, depicting a trend of δD impoverishment at nearly constant $\delta^{18}O$ content. We argued that progressive fluid exsolution at the upper peripheral parts of the AD 79 magma chamber may explain this isotopic trend. This allowed us to propose a schematic model on the pulsed accumulation and release of fluids at the top of the magmatic reservoir prior to the eruption (Figure 5). The observed trend of progressive δD depletion of magmatic fluids released from an active magma chamber, as a consequence of the degassing process, agrees well with the conclusions reported in several previous works on "fossil systems" (e.g., porphyry systems, [39,41,42]) and suggests that this process may be more common than supposed before and does not need very long time to occur. The assessment of the stable isotope composition of the fluids exsolved from the AD 79 magma chamber of Vesuvius can also be particularly relevant for the geochemical surveillance of the volcano, as it may help to interpret the isotopic composition of fumarolic gases and its variations. These are critical parameters in detecting how Vesuvius works and the transitions in its volcanic activity.

Author Contributions: Conceptualization, P.F. and A.J.B.; methodology, P.F. and A.J.B.; validation, P.F. and A.J.B.; formal analysis, A.J.B.; investigation, P.F. and A.J.B.; resources, P.F. and A.J.B.; data curation, A.J.B.; writing—original draft preparation, P.F.; writing—review and editing, P.F. and A.J.B.; visualization, P.F. and A.J.B.; supervision, P.F. and A.J.B.; project administration, P.F. and A.J.B.; funding acquisition, P.F. All authors have read and agreed to the published version of the manuscript.

Funding: This research was funded by the University of Pisa "Fondi di Ateneo 2022" (MUR) to PF.

Data Availability Statement: Not applicable.

Acknowledgments: We warmly thank the technical staff at SUERC for their assistance during the isotope analyses. We also thank the three anonymous reviewers whose comments and suggestions helped to improve the quality of the manuscript.

Conflicts of Interest: The authors declare no conflict of interest.

Appendix A

Hydrogen isotope fractionation models were calculated for: an initial water content of 6.5 wt.% based on analyses of glass inclusions [59]; an initial δD composition of exsolved fluid of –55‰; a H_2O/OH distribution (from 3 to 0.47) for dissolved water based on the speciation model for phonolites of Carroll and Blank [60]; and the H_2O-melt fractionation factor was calculated according to Equation (1) in the text. The closed-system and the open-system trends were calculated by the following equations [51]:

Closed system

$$\delta D_{final} = \delta D_{initial} - (1 - F)\, 1000 \ln\alpha(H_2O\text{-melt})$$

Open system

$$\delta D_{final} = \delta D_{initial} - 1000(1 - F^{\alpha(H_2O\text{-melt})-1})$$

where F is the fraction of H_2O remaining in the melt.

For the "Closed–Open" process we assumed a first stage, in which the exsolution of 50% of the water contained in the melt occurred under closed-system conditions, followed by a second stage of fluid exsolution under open-system conditions. For the "Multi-Step Closed/Open" process we chose a simple 5-step degassing model. Each stage is presumed to exsolve 40% of the water contained in the melt and closed-system degassing describes the isotopic variation of each stage.

References

1. Edmonds, M.; Woods, A.W. Exsolved volatiles in magma reservoirs. *J. Volcanol. Geotherm. Res.* **2018**, *368*, 13–30. [CrossRef]
2. Robock, A. Volcanic eruptions and climate. *Rev. Geophys.* **2000**, *38*, 191–219. [CrossRef]
3. Huppert, H.E.; Woods, A.W. The role of volatiles in magma chamber dynamics. *Nature* **2002**, *420*, 493–495. [CrossRef]
4. Halter, W.E.; Webster, J.D. The magmatic to hydrothermal transition and its bearing on ore-forming systems. *Chem. Geol.* **2004**, *210*, 1–6. [CrossRef]
5. Wilkinson, J.J. Triggers for the formation of porphyry ore deposits in magmatic arcs. *Nat. Geosci.* **2013**, *6*, 917–925. [CrossRef]
6. Hedenquist, J.W.; Lowenstern, J.B. The role of magmas in the formation of hydrothermal ore deposits. *Nature* **1994**, *370*, 519–527. [CrossRef]
7. Audetat, A. The metal content of magmatic-hydrothermal fluids and its relationship to mineralization potential. *Econ. Geol.* **2019**, *114*, 1033–1056. [CrossRef]
8. Kamenetsky, V.S.; Naumov, V.B.; Davidson, P.; Van Achterbergh, E.; Ryan, C.G. Immiscibility between silicate magmas and aqueous fluids: A melt inclusion pursuit into the magmatic-hydrothermal transition in the Omsukchan Granite (NE Russia). *Chem. Geol.* **2004**, *210*, 73–90. [CrossRef]
9. Fischer, T.P.; Chiodini, G. Volcanic, Magmatic and Hydrothermal Gases. In *The Encyclopedia of Volcanoes*, 2nd ed.; Elsevier: Amsterdam, The Netherlands, 2015; pp. 779–797.
10. Roedder, E.; Coombs, D.S. Immiscibility in granitic melts, indicated by fluid inclusions in ejected granitic blocks from Ascension Island. *J. Petrol.* **1967**, *8*, 417–451. [CrossRef]
11. De Vivo, B.; Torok, K.; Ayuso, R.A.; Lima, A.; Lirer, L. Fluid inclusion evidence for magmatic silicate/saline/CO_2 immiscibility and geochemistry of alkaline xenoliths from Ventotene Island, Italy. *Geochim. Cosmochim. Acta* **1995**, *59*, 2941–2953. [CrossRef]

12. Gilg, H.A.; Lima, A.; Somma, R.; Belkin, H.E.; De Vivo, B.; Ayuso, R.A. Isotope geochemistry and fluid inclusion study of skarns from Vesuvius. *Mineral. Petrol.* **2001**, *73*, 145–176. [CrossRef]
13. Fulignati, P.; Kamenetsky, V.S.; Marianelli, P.; Sbrana, A.; Mernagh, T.P. Melt inclusion record of immiscibility between silicate, hydrosaline, and carbonate melts: Applications to skarn genesis at Mount Vesuvius. *Geology* **2001**, *29*, 1043–1046. [CrossRef]
14. Fulignati, P.; Marianelli, P.; Santacroce, R.; Sbrana, A. Probing the Vesuvius magma chamber-host rock interface through xenoliths. *Geol. Mag.* **2004**, *141*, 417–428. [CrossRef]
15. Fulignati, P.; Marianelli, P.; Proto, M.; Sbrana, A. Evidences for disruption of a crystallizing front in a magma chamber during caldera collapse: An example from the Breccia Museo unit (Campanian Ignimbrite eruption, Italy). *J. Volcanol. Geotherm. Res.* **2004**, *133*, 141–155. [CrossRef]
16. Fulignati, P.; Panichi, C.; Sbrana, A.; Caliro, S.; Gioncada, A.; Del Moro, A. Skarn formation at the walls of the 79AD magma chamber of Vesuvius (Italy): Mineralogical and isotopic constraints. *Neues Jahrb. Für. Mineral. Abh.* **2005**, *181*, 53–66. [CrossRef]
17. Fulignati, P.; Kamenetsky, V.S.; Marianelli, P.; Sbrana, A.; Meffre, S. First insights on the metallogenic signature of magmatic fluids exsolved from the active magma chamber of Vesuvius (AD 79 "Pompei" eruption). *J. Volcanol. Geotherm. Res.* **2011**, *200*, 223–233. [CrossRef]
18. Sbrana, A.; Fulignati, P.; Marianelli, P.; Boyce, A.J.; Cecchetti, A. Exhumation of an active magmatic-hydrothermal system in a resurgent caldera environment: The example of Ischia (Italy). *J. Geol. Soc. Lond.* **2009**, *166*, 1061–1073. [CrossRef]
19. Barberi, F.; Leoni, L. Metamorphic carbonate ejecta from Vesuvius plinian eruptions: Evidence of the occurrence of shallow magma chambers. *Bull. Volcanol.* **1980**, *43*, 107–120. [CrossRef]
20. Cioni, R.; Civetta, L.; Marianelli, P.; Metrich, N.; Santacroce, R.; Sbrana, A. Compositional layering and syn-eruptive mixing of a periodically refilled shallow magma chamber: The AD 79 Plinian eruption of Vesuvius. *J. Petrol.* **1995**, *36*, 739–776. [CrossRef]
21. Cioni, R.; Marianelli, P.; Santacroce, R. Thermal and compositional evolution of the shallow magma chambers of Vesuvius: Evidence from pyroxene phenocrysts and melt inclusions. *J. Geophys. Res.* **1998**, *103*, 18277–18294. [CrossRef]
22. Cioni, R.; Santacroce, R.; Sbrana, A. Pyroclastic deposits as a guide for reconstructing the multi-stage evolution of the Somma-Vesuvius Caldera. *Bull. Volcanol.* **1999**, *60*, 207–222. [CrossRef]
23. Marsh, B.D. Solidification fronts and magmatic evolution. *Mineral. Mag.* **1995**, *60*, 5–40. [CrossRef]
24. Sharp, Z.D. A laser-based microanalytical method for the in situ determination of oxygen isotope ratios in silicates and oxides. *Geochim. Cosmochim. Acta* **1990**, *54*, 1353–1357. [CrossRef]
25. Donnelly, T.; Waldron, S.; Tait, A.; Dougans, J.; Bearhop, S. Hydrogen isotope analysis of natural abundance and deuterium-enriched waters by reduction over chromium on-line to a dynamic dual inlet isotope-ratio mass spectrometer. *Rapid. Commun. Mass Spectrom.* **2001**, *15*, 1297–1303. [CrossRef]
26. Ayuso, R.A.; De Vivo, B.; Rolandi, G.; Seal, R.R.; Paone, A. Geochemical and isotopic (Nd-Pb-Sr-O) variations bearing on the genesis of volcanic rocks from Vesuvius, Italy. *J. Volcanol. Geotherm. Res.* **1998**, *82*, 53–78. [CrossRef]
27. Iovine, R.S.; Mazzeo, F.C.; Worner Pelullo, C.; Cirillo, G.; Arienzo, I.; Pack, A.; D'Antonio, M. Coupled δ^{18}O-δ^{17}O and ^{87}Sr/^{86}Sr isotope compositions suggest a radiogenic and ^{18}O-enriched magma source for Neapolitan volcanoes (Southern Italy). *Lithos* **2018**, *316–317*, 199–211. [CrossRef]
28. Zheng, Y.F. Calculation of oxygen isotope fractionation in anhydrous silicate minerals. *Geochim. Cosmochim. Acta* **1993**, *57*, 1079–1091. [CrossRef]
29. Zheng, Y.F. Calculation of oxygen isotope fractionation in hydroxyl-bearing minerals. *Earth Planet. Sci. Lett.* **1993**, *120*, 247–263. [CrossRef]
30. Suzuoki, T.; Epstein, S. Hydrogen isotope fractionation between OH-bearing minerals and water. *Geochim. Cosmochim. Acta* **1976**, *40*, 1229–1240. [CrossRef]
31. Sheppard, S.M.F.; Nielsen, R.L.; Taylor, H.P., Jr. Oxygen and hydrogen isotope ratios of clay minerals from porphyry copper deposits. *Econ. Geol.* **1969**, *64*, 755–777. [CrossRef]
32. Taylor, H.P., Jr. The application of oxygen and hydrogen isotope studies to problems of hydrothermal alteration and ore deposition. *Econ. Geol.* **1974**, *69*, 843–883. [CrossRef]
33. D'Amore, F.; Bolognesi, L. Isotopic evidence for a magmatic contribution to fluids of the geothermal systems of Larderello, Italy, and The Geyser, California. *Geothermics* **1994**, *23*, 21–32. [CrossRef]
34. Goff, F.; McMurtry, G.M. Tritium and stable isotopes in magmatic waters. *J. Volcanol. Geotherm. Res.* **2000**, *97*, 347–396. [CrossRef]
35. Taylor, H.P., Jr.; Sheppard, S.M.F. Igneous Rocks: I. Processes of Isotopic Fractionation and Isotope Systematics. In *Stable Isotopes in High Temperature Geological Processes*; Valley, J.W., Taylor, H.P., Jr., O'Neil, J.R., Eds.; De Gruyter: Berlin, Cermany, 1986; Volume 16, pp. 227–271.
36. O'Neil, J.R.; Taylor, H.P., Jr. The oxygen isotope and cation exchange chemistry of feldspars. *Am. Mineral.* **1967**, *52*, 1414–1437.
37. Bottinga, Y.; Javoy, M. Comments on oxygen isotope geothermometry. *Earth Planet. Sci. Lett.* **1973**, *20*, 250–265. [CrossRef]
38. Bottinga, Y.; Javoy, M. Oxygen isotope partitioning among the minerals in igneous and metamorphic rocks. *Rev. Geophys. Space Phys.* **1975**, *13*, 401–418. [CrossRef]
39. Sheppard, S.M.F. Characterization and Isotopic Variations in Natural Waters. In *Stable Isotopes in High Temperature Geological Processes*; Valley, J.W., Taylor, H.P., Jr., O'Neil, J.R., Eds.; De Gruyter: Berlin, Cermany, 1986; Volume 16, pp. 165–183.

40. Taylor, B.E. Degassing of H_2O from Rhyolite Magma During Eruption and Shallow Intrusion, and the Isotopic Composition of Magmatic Water in Hydrothermal Systems. In *Magmatic Contribution to Hydrothermal Systems*; Hedenquist, J.W., Ed.; Geological Survey of Japan Report: Tsukuba, Japan, 1992; Volume 279, pp. 190–194.
41. Hedenquist, J.W.; Arribas, A.; Reynolds, T.J. Evolution of an Intrusion-Centered Hydrothermal System: Far Southeast-Lepanto Porphyry and Epithermal Cu-Au Deposits, Philippines. *Econ. Geol.* **1998**, *93*, 373–404. [CrossRef]
42. Harris, A.C.; Golding, S.D. New evidence of magmatic-fluid-related phyllic alteration: Implications for the genesis of porphyry Cu deposits. *Geology* **2002**, *30*, 335–338. [CrossRef]
43. Meinert, L.D.; Hedenquist, J.W.; Satoh, H.; Matsuhisa, Y. Formation of anhydrous and hydrous skarn in Cu-Au ore deposits by magmatic fluids. *Econ. Geol.* **2003**, *98*, 147–156. [CrossRef]
44. Harris, A.C.; Golding, S.D.; White, N.C. Bajo de la Alumbrera copper-gold deposit: Stable isotope evidence for a porphyry-related hydrothermal system dominated by magmatic aqueous fluids. *Econ. Geol.* **2005**, *100*, 863–888. [CrossRef]
45. Taylor, B.E.; Eichelberger, J.C.; Westrich, H.R. Hydrogen isotopic evidence for rhyolitic magma degassing during shallow intrusion and eruption. *Nature* **1983**, *306*, 541–545. [CrossRef]
46. Javoy, M. Stable isotopes and geothermometry. *J. Geol. Soc. Lond.* **1977**, *133*, 603–636. [CrossRef]
47. Horita, J.; Cole, D.R.; Wesolowski, D.J. The activity-composition relationship of oxygen and hydrogen isotopes in aqueous salt solutions: III. Vapor-liquid water equilibration of NaCl solution to 350 °C. *Geochim. Cosmochim. Acta* **1995**, *59*, 1139–1151. [CrossRef]
48. Shmulovich, K.I.; Landwehr, D.; Simon, K.; Heinrich, W. Stable isotope fractionation between liquid and vapor in water-salt systems up to 600 °C. *Chem. Geol.* **1999**, *157*, 343–354. [CrossRef]
49. Dobson, P.F.; Epstein, S.; Stolper, E.M. Hydrogen isotope fractionation between coexisting vapor and silicate glasses and melts at low pressure. *Geochim. Cosmochim. Acta* **1989**, *53*, 2723–2730. [CrossRef]
50. Taylor, B.E. Magmatic Volatiles: Isotopic Variation of C, H, and S. In *Stable Isotopes in High Temperature Geological Processes*; Valley, J.W., Taylor, H.P., Jr., O'Neil, J.R., Eds.; De Gruyter: Berlin, Cermany, 1986; Volume 16, pp. 185–225.
51. Taylor, B.E. Degassing of Obsidian Dome Rhyolite, Inyo Volcanic Chain, California. In *Stable Isotope Geochemistry: A Tribute to Samuel Epstein*; Taylor, H.P., Jr., O'Neil, J.R., Kaplan, I.R., Eds.; Geochemical Society: Washington, DC, USA, 1991; Volume 3, pp. 339–353.
52. Newman, S.; Epstein, S.; Stolper, E.M. Water, carbon dioxide, and hydrogen isotopes in glasses from the ca.1340A.D. eruption of the Mono Craters, California: Constraints on degassing phenomena and initial volatile content. *J. Volcanol. Geotherm. Res.* **1988**, *35*, 75–96. [CrossRef]
53. Barnes, J.D.; Prather, T.J.; Cisneros, M.; Befus, K.; Gardner, J.E.; Larson, T.E. Stable chlorine isotope behavior during volcanic degassing of H_2O and CO_2 at Mono Craters, CA. *Bull. Volcanol.* **2014**, *76*, 805. [CrossRef]
54. Burnham, C.W. Energy release in subvolcanic environments: Implications for breccia formation. *Econ. Geol.* **1985**, *80*, 1515–1522. [CrossRef]
55. Shinohara, H.; Kazahaya, K. Degassing Processes Related to Magma-Chamber Crystallization. In *Magmas, Fluids, and Ore Deposits*; Thompson, J.F.H., Ed.; Mineralogical Association of Canada: Québec, QC, Canada, 1995; Volume 23, pp. 47–70.
56. Fournier, R.O. Hydrothermal processes related to movement of fluid from plastic into brittle rock in the magmatic-epithermal environment. *Econ. Geol.* **1999**, *94*, 1193–1212. [CrossRef]
57. Li, Y.; Li, X.-H.; Selby, D.; Li, J.-W. Pulsed magmatic fluid release for the formation of porphyry deposits: Tracing fluid evolution in absolute time from Tibetan Qulong Cu-Mo deposit. *Geology* **2018**, *46*, 7–10. [CrossRef]
58. Bain, W.M.; Lecumberri-Sanchez, P.; Marsh, E.E.; Steele-MacInnis, M. Fluids and melts at the magmatic-hydrothermal transition, recorded by unidirectional solidification textures at Saginaw Hil, Arizona, USA. *Econ. Geol.* **2022**, *117*, 1543–1571. [CrossRef]
59. Cioni, R. Volatile content and degassing processes in the AD 79 magma chamber at Vesuvius (Italy). *Contrib. Mineral. Petrol.* **2000**, *140*, 40–54. [CrossRef]
60. Carroll, M.R.; Blank, J.G. The solubility of H_2O in phonolitic melts. *Am. Mineral.* **1997**, *82*, 549–556. [CrossRef]